Science of the Total Environment 799 (2021) 149416

Contents lists available at ScienceDirect

Science of the Total Environment

journal homepage: www.elsevier.com/locate/scitotenv

Seasonal variations of nutrient concentrations and their ratios in the central Bohai Sea

Xiaokun Ding [a,b], Xinyu Guo [a,b,*], Huiwang Gao [a,c], Jie Gao [b], Jie Shi [a,c], Xiaojie Yu [a], Zhaosen Wu [a]

[a] Frontiers Science Center for Deep Ocean Multispheres and Earth System, Key Laboratory of Marine Environment and Ecology, Ministry of Education of China, Ocean University of China, 238 Songling Road, Qingdao 266100, China
[b] Center for Marine Environmental Studies, Ehime University, 2-5 Bunkyo-Cho, Matsuyama 790-8577, Japan
[c] Laboratory for Marine Ecology and Environmental Sciences, Qingdao National Laboratory for Marine Science and Technology, Qingdao 266071, China

HIGHLIGHTS

- Apparent seasonal variations appeared in nutrient concentrations and the N/P ratio.
- A pelagic–benthic coupled model was designed to quantify the influence mechanisms.
- Biological processes controlled the seasonal variation of nutrients.
- External inputs alleviated nutrient limitation in summer.
- Variation of N/P ratio of phytoplankton uptake affected the nitrate concentration.

GRAPHICAL ABSTRACT

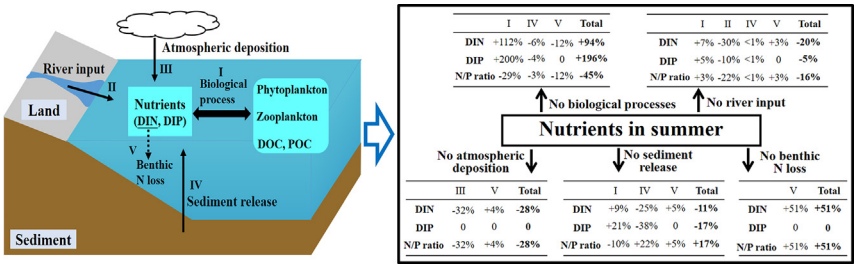

ARTICLE INFO

Article history:
Received 5 April 2021
Received in revised form 17 July 2021
Accepted 29 July 2021
Available online 3 August 2021

Editor: Ouyang Wei

Keywords:
Seasonal variation
Nutrient ratio
External inputs
Biological process
Central Bohai Sea

ABSTRACT

The Bohai Sea is a typical semi-enclosed sea in the northwest Pacific, which is subject to serious eutrophication due to human activities. Similar to hydrographic variables such as water temperature and salinity, the nutrient concentrations and ratios in the Bohai Sea also exhibit seasonal variations. However, the effects of external inputs, biological processes, and benthic processes on these seasonal variations have not been quantified to date. To address this issue, a physical–biological coupled model was developed to capture the seasonal nutrient cycling in the central Bohai Sea. The simulation results revealed apparent seasonal variations in the concentrations of dissolved inorganic nitrogen (DIN), dissolved inorganic phosphorus (DIP), and dissolved silicate (DSi). The N/P ratio (as the molar ratio of DIN/DIP) also exhibited an apparent seasonal variation, with the maximum and minimum values in surface water occurring in summer (>100) and winter (<30), respectively. The Si/N ratio (as the molar ratio of DSi/DIN) was slightly higher in summer than in other seasons. The budget for three types of nutrient indicated that the biological processes determined the seasonal variations in nutrient concentrations and the N/P ratio. The external inputs of nutrients via river input, atmospheric deposition, and sediment release were probably important in summer when they could alleviate the reduced nutrient concentrations due to biological processes. To maintain a reasonable nitrogen budget, it was necessary to include benthic nitrogen loss, which removed a large amount of inorganic nitrogen in summer and autumn. In addition, the variation of N/P ratio of phytoplankton uptake can reduce the ratio of DIN to DIP in surface water by ~20 in summer as compared to the calculation with a fixed N/P ratio (16:1) in phytoplankton uptake.

* Corresponding author at: Frontiers Science Center for Deep Ocean Multispheres and Earth System, Key Laboratory of Marine Environment and Ecology, Ministry of Education of China, Ocean University of China, 238 Songling Road, Qingdao 266100, China.
E-mail address: guoxinyu@sci.ehime-u.ac.jp (X. Guo).

https://doi.org/10.1016/j.scitotenv.2021.149416
0048-9697/

1. Introduction

Nutrients including dissolved inorganic nitrogen (DIN), dissolved inorganic phosphorus (DIP), and dissolved silicate (DSi) are necessary for phytoplankton growth, whose primary productivity is the basis of the marine ecosystem (Bristow et al., 2017). Increasing human activity increases the external input of nutrients into coastal regions and sometimes causes an over-enriched state of nutrients (i.e., eutrophication) (Kim et al., 2011; Song et al., 2016). Over-enriched nutrient conditions lead to some environmental issues, such as the frequent occurrence of harmful algal blooms and jellyfish blooms, changes in plankton community structure, and ocean acidification (Zhou et al., 2018; Wang et al., 2018a).

Similar to hydrographic variables such as water temperature and salinity, the nutrient concentrations in many coastal seas exhibit seasonal variations, which have been widely reported to be associated with a variety of external factors and local biogeochemical processes. For example, the nutrient concentrations in the Bay of Bengal were higher during the northeast monsoon season than those during other seasons because of the large anthropogenic nutrient load (Achary et al., 2014). The nitrate concentration was high in spring in the coastal waters of Namibia due to strong Benguela upwelling (Louw et al., 2016). Similarly, the increase in nutrient concentrations off the northern Galician coast in summer was found to be associated with upwelling events (Caseas et al., 1997). On the other hand, the uptake of nutrients by phytoplankton in spring and summer was also suggested to be the cause of the lowest nutrient concentrations in the Seto Inland Sea (Yamaguchi et al., 2020), southeastern Mediterranean Sea (Herut et al., 2000), and the Baltic Sea (Lyngsgaard et al., 2017; Purina et al., 2018).

Nutrient ratios vary widely in nutrient-related processes. Compared with the fixed Redfield ratio (16:1) of nitrogen to phosphorus in the ocean (Redfield, 1934), there is excess nitrogen relative to phosphorus in riverine input (Liu et al., 2009; Ounissi et al., 2018) and atmospheric deposition (Shi et al., 2012). This excess nitrogen in coastal waters induces an N/P ratio (as the molar ratio of DIN/DIP) of >16 (Macias et al., 2019). Naturally, with the seasonal variation in nutrient concentrations, nutrient ratios also show a seasonal variation (Fisher et al., 1992; Fan and Song, 2014).

The Bohai Sea is a typical semi-enclosed shallow sea in the northwest Pacific, which is subject to serious eutrophication (Song et al., 2016; Xin et al., 2019). Many field surveys have documented seasonal variations in the concentrations and ratios of nutrients in the Bohai Sea (J.J. Wang et al., 2019; Zheng et al., 2020). In general, nutrient concentrations have exhibited maximum values in winter and minimum values in summer in recent years (Sui et al., 2016; Zhou et al., 2018). The highest N/P ratio is in summer, when its value exceeds the Redfield ratio of 16:1, while the Si/N ratio (as the molar ratio of DSi/DIN) is slightly higher in summer than in other seasons (Sui et al., 2016; J.J. Wang et al., 2019). The extremely high N/P ratio in summer is probably a cause of the drastic changes in the composition of the plankton community (Chen et al., 2016; Y.B. Wang et al., 2019), as well as the frequent occurrence of harmful algal blooms (Song et al., 2016) and hypoxia (Zhai et al., 2019), which further induce a decline in the fishery resources of the Bohai Sea (Zhang et al., 2012).

The Bohai Sea has been reported to have received >30% of mainland China's total marine pollution, although it only constitutes <3% of the total marine area of China (Xin et al., 2019). Many studies have emphasized the important impact of external inputs on the nutrient budget of the Bohai Sea, including river input (Liu, 2015; Ding et al., 2020), atmospheric deposition (Shou et al., 2018; Qi et al., 2020), nutrient release from sediments (Liu et al., 2011; Mu et al., 2017), inputs from the Yellow Sea (Zheng et al., 2020), and non-point sources (Liu et al., 2017; J.J. Wang et al., 2019). In recent years, these excessive nutrient loads have led to high phytoplankton biomass in the Bohai Sea, especially in summer (Ding et al., 2020). Naturally, phytoplankton-related biological processes also affect nutrient concentrations in seawater. To date, there is no literature addressing the quantitative impacts of external inputs and local biological processes on the seasonal variations in nutrient concentrations and ratios in the Bohai Sea.

The purpose of this study is to quantitatively examine the impacts of various biogeochemical processes on the seasonal variations in nutrient concentrations and ratios in the central Bohai Sea (CBS) region. Accordingly, we developed a 1D physical–biological coupled model to describe the seasonal nutrient cycling over the CBS. A series of numerical experiments were designed to analyze the impacts of multiple factors on the seasonal variations of nutrient concentrations and ratios.

2. Methodology

2.1. Study area

The Bohai Sea (37°10′–41°10′ N, 117°35′–122°10′ E) has an average depth of 18 m and a total area of 7.7×10^4 km^2 (Fig. 1), and is connected to the Yellow Sea through the Bohai Strait. Based on geographical location, the sea is usually divided into five areas: Liaodong Bay, Bohai Bay, Laizhou Bay, Qinhuangdao coast, and the CBS (Zhang et al., 2017). Nutrients in coastal areas have been reported to be affected by non-point emissions, such as sewage discharge and extensive aquaculture (J.J. Wang et al., 2019; Xin et al., 2019). However, the necessary high-resolution coastal non-point source emissions data over the entire Bohai Sea is not available. Therefore, we have to select the CBS as our study area, where coastal non-point source emissions affect little the nutrients concentration there (Li et al., 2015; J.J. Wang et al., 2019). The CBS has an area of 2.9×10^4 km^2 and an average depth of 22.5 m. The phytoplankton biomass in the CBS accounts for nearly half of that in the entire Bohai Sea (Ding et al., 2020). Therefore, clarifying the seasonal variations of nutrient concentrations in the CBS is helpful for understanding the nutrient cycle in the entire Bohai Sea.

2.2. Model description

A vertical 1D physical–biological coupled model was implemented to analyze the nutrient dynamics in the CBS. The model was composed of three sub-models: a hydrodynamic model, pelagic biological model, and benthic model. There were 40 layers in the vertical direction. The hydrodynamic model was based on the 1D Princeton Ocean Model (Blumberg and Mellor, 1987), which provided the water temperature and diffusivity coefficient for the biological model. A detailed description and validation of the hydrodynamic model for the CBS are available in Ding et al. (2020).

We developed a pelagic biological model describing the complex processes of the planktonic ecosystem based on the North Pacific Ecosystem Model for Understanding Regional Oceanography (NEMURO) (Kishi et al., 2007). As shown in Fig. 2, there are 14 state variables: two types of DIN (nitrate (NO_3^-) and ammonium (NH_4^+)), DIP, DSi, dinoflagellates (PS), diatoms (PL), two types of zooplankton (microzooplankton (ZS) and mesozooplankton (ZL)), bacteria, dissolved organic nitrogen (DON), dissolved organic phosphorus (DOP), particulate organic nitrogen (PON), particulate organic phosphorus (POP), and biogenic silica (BSi). The governing equations and formulations of various biogeochemical processes are given in Text S1, and a list of the parameters used in the model is provided in Table S1.

The benthic model was based on the work of Capet et al. (2016), and included three types of organic matter (PON, POP, and BSi). It describes the sedimentary accumulation, decomposition, and burial of organic matter leaving the water column. All benthic variables were depth-integrated and expressed in mmol m^{-2}. The model equations are presented in Text S2, and the parameter values are listed in Table S2. The pelagic model provided the input flux of organic matter into the benthic layer. After calculating the accumulation, decomposition, and burial of organic matter within the benthic layer, the benthic model

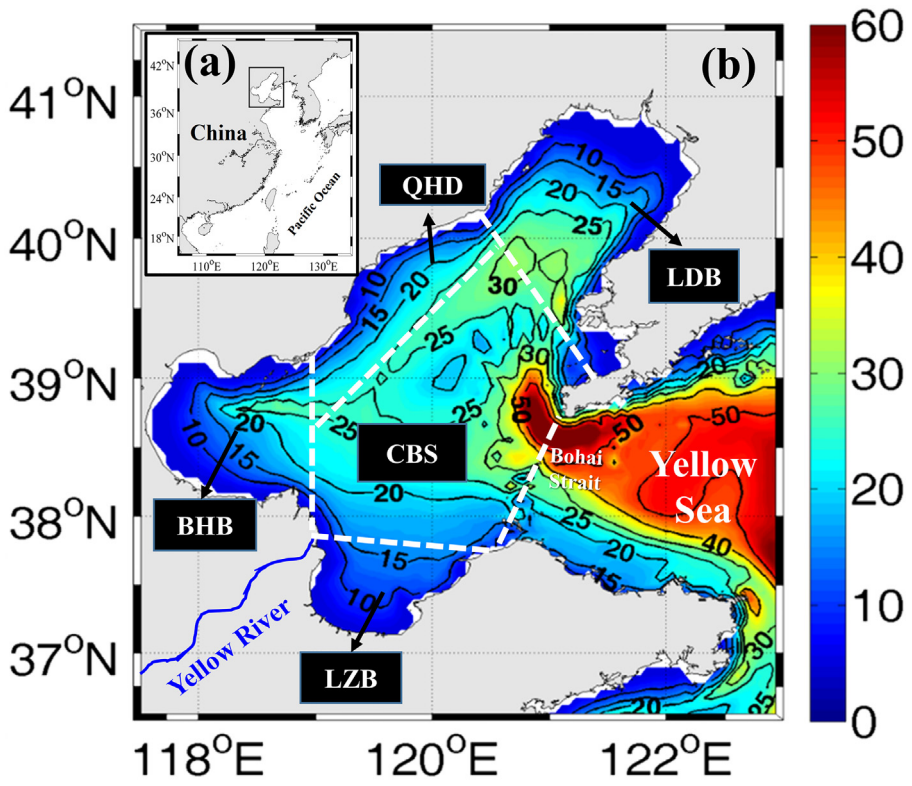

Fig. 1. (a) Location of the Bohai Sea, and (b) study area and bathymetry (contour lines, units in meters). The sea is divided into five subregions by white dashed lines: Liaodong Bay (LDB), Qinhuangdao coast (QHD), Bohai Bay (BHB), Laizhou Bay (LZB), and the central Bohai Sea (CBS).

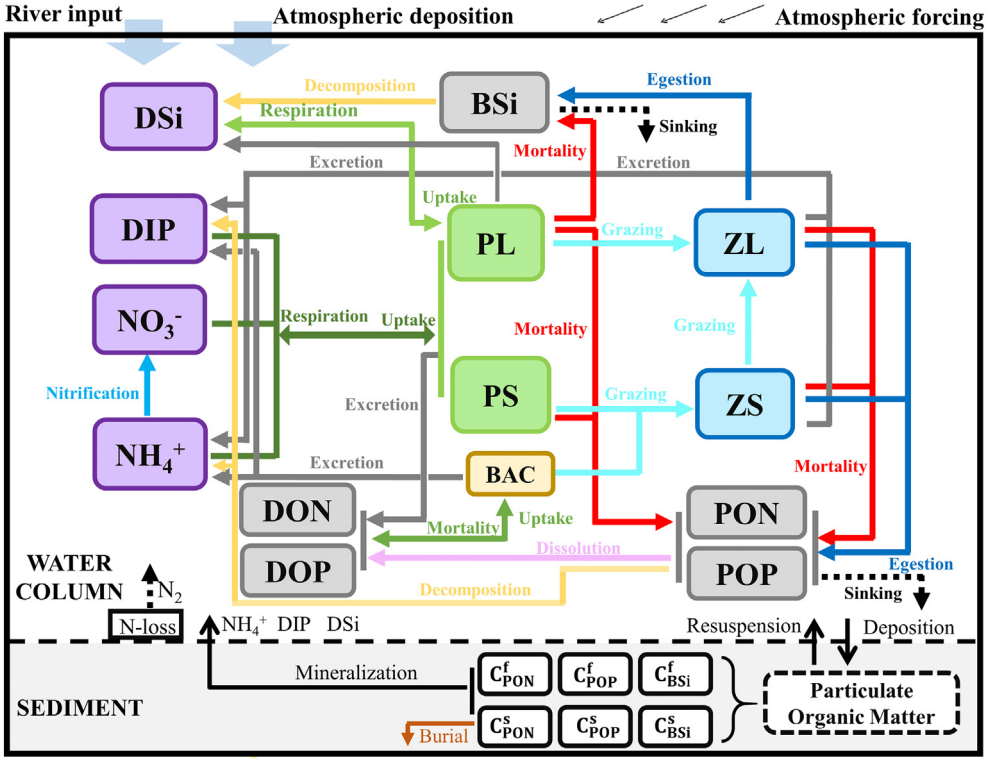

Fig. 2. Schematic of the pelagic–sediment coupled model. The pelagic model includes 14 state variables: nitrate (NO_3^-), ammonium (NH_4^+), dissolved inorganic phosphorus (DIP), dissolved silicate (DSi), dinoflagellates (PS), diatoms (PL), microzooplankton (ZS), mesozooplankton (ZL), bacteria (BAC), dissolved organic nitrogen (DON), dissolved organic phosphorus (DOP), particulate organic nitrogen (PON), particulate organic phosphorus (POP), and biogenic silica (BSi). The benthic model includes six state variables: fast decaying PON (C^f_{PON}), POP (C^f_{POP}), and BSi (C^f_{BSi}), and slow decaying PON (C^s_{PON}), POP (C^s_{POP}), and BSi (C^s_{BSi}). The colored solid lines represent different biogeochemical processes corresponding to the words shown in the same color. (For interpretation of the references to color in this figure legend, the reader is referred to the web version of this article.)

subsequently provided the sediment–water fluxes of nutrients, which were the bottom boundary conditions for nutrients in the pelagic model.

2.3. Model configuration

The hydrodynamic model was initialized with the temperature and salinity data in January and driven by climatological monthly atmospheric forcing, which was described in detail by Ding et al. (2020). Here we only give the detailed configurations of the pelagic biological model and benthic model.

2.3.1. Nutrient input from boundaries

The Yellow River is the second-largest river in China, and accounts for >75% of the total river discharge into the Bohai Sea (Liu and Yin, 2010). The nutrients carried by the diluted water of the Yellow River can be transported into the CBS, especially in summer owing to the southeasterly wind (Wang et al., 2008), thereby playing an important role in primary production (Ding et al., 2020). The nutrient carried by the small rivers into the sea usually stays along the coastal line because its small river discharge cannot form a bulge that is a necessary condition for an offshore transport of river water (Yu et al., 2020). Consequently, the nutrients from the small rivers affect little the ecosystem of the central waters (Li et al., 2015; Ding et al., 2020). Thus, the nutrients from the Yellow River were considered to be the only riverine nutrient input in this study. The riverine nutrient input in the model consisted of the long-term averaged (2008–2017) monthly fluxes of DIN, DIP, DSi, DOP, and particulate phosphorus (PP), which were calculated according to the regression relationships between nutrient fluxes and river discharge (Liu, 2015). As shown in Fig. S1a, the highest riverine nutrient fluxes occurred in summer. Particulate nitrogen and silicon were not considered in the model because their fluxes were very low compared to those of dissolved nitrogen and silicon (Liu et al., 2009; Wang et al., 2012). The nutrients from the Yellow River exist mainly in its diluted water that moves with the current. Therefore, the proportion of the nutrient flux from the Yellow River into the CBS was assumed to be the proportion of water flux transported from the estuary into the CBS without considering the consumption of nutrients during their transportation to the CBS (Ding et al., 2020). Moreover, the riverine PP was assumed to be decomposed into DOP and DIP in the estuary, which were then transported into the CBS. The proportions of PP decomposed into DOP (~4.8%) and DIP (~11.2%) were obtained from He et al. (2010). The calculated riverine fluxes of nutrients into the CBS are shown in Fig. S1b.

According to previous studies, atmospheric nitrogen deposition is 1.1–1.5 times higher than that from major rivers in the Bohai Sea, Yellow Sea, and East China Sea (Zhang et al., 2010; Shou et al., 2018; Qi et al., 2020). In this study, the monthly atmospheric deposition fluxes of NO_3^- and NH_4^+ in the CBS were obtained from an atmospheric transport model (Guo, 2019; Fig. S1c). In this study, we did not consider the atmospheric phosphorus deposition since the phosphorus flux from atmospheric deposition is extremely low in the Bohai Sea (Shi et al., 2012; J.J. Wang et al., 2019).

In addition, the nutrient fluxes between the CBS and the Yellow Sea were estimated to be much smaller than the riverine nutrient fluxes; hence, they were not considered in the model (see Text S3 for details).

2.3.2. Initial conditions and calculation

The observational data collected in winter over the CBS (Table S3) were averaged to provide the initial vertical profiles of DIN, DIP, and DSi concentrations. Other pelagic biological variables, including phytoplankton, zooplankton, and other organic matter, were initially set to a homogeneous small value of 0.1 mmol m^{-3} (Fennel et al., 2006). In addition, the benthic variables were initiated based on the simulated results for January over the Bohai Sea from a pelagic–benthic coupled model (Zhang et al., 2006). The initial values of inorganic nutrients in water and particulate matters in sediment were listed in Table S4.

The physical and biological variables were simultaneously calculated at a time step of 216 s. The model was integrated for five years with climatological surface forcing and monthly nutrient inputs. The first four years were for the model spin-up; thus, we chose the simulated results of the fifth year for the analysis.

2.4. Numerical experiment

To examine the impacts of various factors on the seasonal variations in nutrients, we designed a series of numerical experiments after the model spin-up period (Table 1). Case 0 was the realistic (control) case mentioned in Section 2.3. Case 1 was used to investigate the effects of biological processes by removing all biological processes in seawater. Cases 2 and 3 were used to examine the effects of river input and atmospheric deposition, respectively. Case 4 was used to investigate the effect of sediment nutrient release by closing the nutrient supply from the sediment–water interface. Case 5 was used to examine the effect of benthic nitrogen loss by setting the benthic nitrogen removal rate to 0. Finally, Case 6 was used to investigate the effects of the variation of N/P ratio in phytoplankton uptake used in Case 0 by fixing the N/P ratio in phytoplankton uptake to 16 (=the Redfield ratio).

In the model, the temporal variation rate of the nutrient inventory for a unit area was expressed by:

$$\frac{d}{dt}\int_{-h}^{0} C(z)dz = \int_{-h}^{0} Bio(z)dz + Riv + Atm + Sed + NL, \quad (1)$$

where h is the water depth, $C(z)$ denotes the nutrient concentration at depth (z), $Bio(z)$ represents the biological processes, Riv is the river input, Atm is the atmospheric deposition of DIN, Sed is the nutrient release from sediments, and NL is the benthic nitrogen loss. To determine the effects of each process on the nutrient inventory, we calculated the difference for each term on the right-hand side of Eq. (1) between Cases 1 to 5 and Case 0 (i.e., the control):

$$\begin{bmatrix} \Delta NF_i^j(t) = NF_i^0(t) - NF_i^j(t) \\ \Delta PF_i^j(t) = PF_i^0(t) - PF_i^j(t) \end{bmatrix}, \quad (2)$$

where NF and PF represent the terms in Eq. (1) for DIN and DIP, respectively; i (=I, II, III, IV, or V) is the index for the five terms on the right-hand side of Eq. (1) and j (=1, 2, 3, 4, or 5) is the index for Cases 1–5.

Table 1
List of numerical experiments. "+" and "−" indicate that the process was included and excluded in the simulated case, respectively (see Section 2.4 for details).

	Biological processes	River input	Atmospheric deposition	Sediment nutrients release	Benthic N loss	Non-Redfield ratio
Case 0	+	+	+	+	+	+
Case 1	−	+	+	+	+	+
Case 2	+	−	+	+	+	+
Case 3	+	+	−	+	+	+
Case 4	+	+	+	−	+	+
Case 5	+	+	+	+	−	+
Case 6	+	+	+	+	+	−

Accordingly, NF_i^0 and PF_i^0 are the DIN and DIP fluxes of each process in Eq. (1) for Case 0, while NF_i^j and PF_i^j are the DIN and DIP fluxes of each process in Eq. (1) for Cases 1–5.

We defined the change in nutrient concentrations due to ΔNF_i^j as ΔDIN_i^j, and that due to ΔPF_i^j as ΔDIP_i^j:

$$\begin{cases} \Delta DIN_i^j(t) = \frac{1}{h}\int_0^t \Delta NF_i^j(t)dt \\ \Delta DIP_i^j(t) = \frac{1}{h}\int_0^t \Delta PF_i^j(t)dt \end{cases}, \quad (3)$$

where h is the water depth.

To evaluate the contributions of ΔNF_i^j or ΔPF_i^j to the change in nutrient concentrations and ratios, we calculated the ratios of the nutrient concentrations and N/P ratio change due to ΔNF_i^j (or ΔPF_i^j) to the corresponding values in Case 0, as expressed by:

$$\begin{cases} RN_i^j(t) = -\Delta DIN_i^j(t)/DIN^0(t) \\ RP_i^j(t) = -\Delta DIP_i^j(t)/DIP^0(t) \\ RNP_i^j(t) = \left(\frac{DIN^0(t)-\Delta DIN_i^j(t)}{DIP^0(t)-\Delta DIP_i^j(t)} - \frac{DIN^0(t)}{DIP^0(t)}\right) / \frac{DIN^0(t)}{DIP^0(t)} \end{cases}, \quad (4)$$

where i and j are the same as those described in Eq. (2), and DIN^0 and DIP^0 are the simulated DIN and DIP concentrations in Case 0, respectively.

2.5. Calculation of nutrients conversion time

Based on the nutrient inventory and fluxes of different processes in seawater, the conversion time (γ) of nutrients for the different processes was calculated as follows:

$$\gamma = \frac{\int_{-h}^{0} Nut(z)dz}{F_s}, \quad (5)$$

where Nut represents the nutrient concentrations at depth z; F_s denotes the nutrient fluxes corresponding to one process; and h is the water depth.

3. Results

3.1. Seasonal variations in nutrient concentrations

The vertical profiles of the simulated nutrient concentrations in each season were generally within the range of observational data (Fig. S3), indicating that the model could simulate the seasonal variations in the vertical distributions of nutrients in the CBS. Fig. 3 displayed the vertical distributions of simulated DIN, DIP, and DSi in winter (January, February, and March), spring (April, May, and June), summer (July, August, and September), and autumn (October, November, and December). The lowest and highest concentrations of these three dissolved nutrients were in summer and winter, respectively, while spring and autumn were the transitional periods between these two extreme concentrations. The vertical mean concentrations of nutrients in winter, spring, summer, and autumn were 15.7 mmol m^{-3}, 12.9 mmol m^{-3}, 8.7 mmol m^{-3}, and 12.4 mmol m^{-3} for DIN, respectively; 0.6 mmol m^{-3}, 0.4 mmol m^{-3}, 0.2 mmol m^{-3}, and 0.4 mmol m^{-3} for DIP, respectively; and 17.1 mmol m^{-3}, 14.6 mmol m^{-3}, 12.5 mmol m^{-3}, and 15.6 mmol m^{-3} for DSi, respectively. The summertime nutrient concentrations were significantly lower in surface water (~8.5 mmol DIN m^{-3}, <0.1 mmol DIP m^{-3}, and ~10 mmol DSi m^{-3}) than those in bottom water (~9.5 mmol DIN m^{-3}, >0.3 mmol DIP m^{-3}, and ~15 mmol DSi m^{-3}), while almost no vertical variation was observed in the wintertime nutrient concentrations.

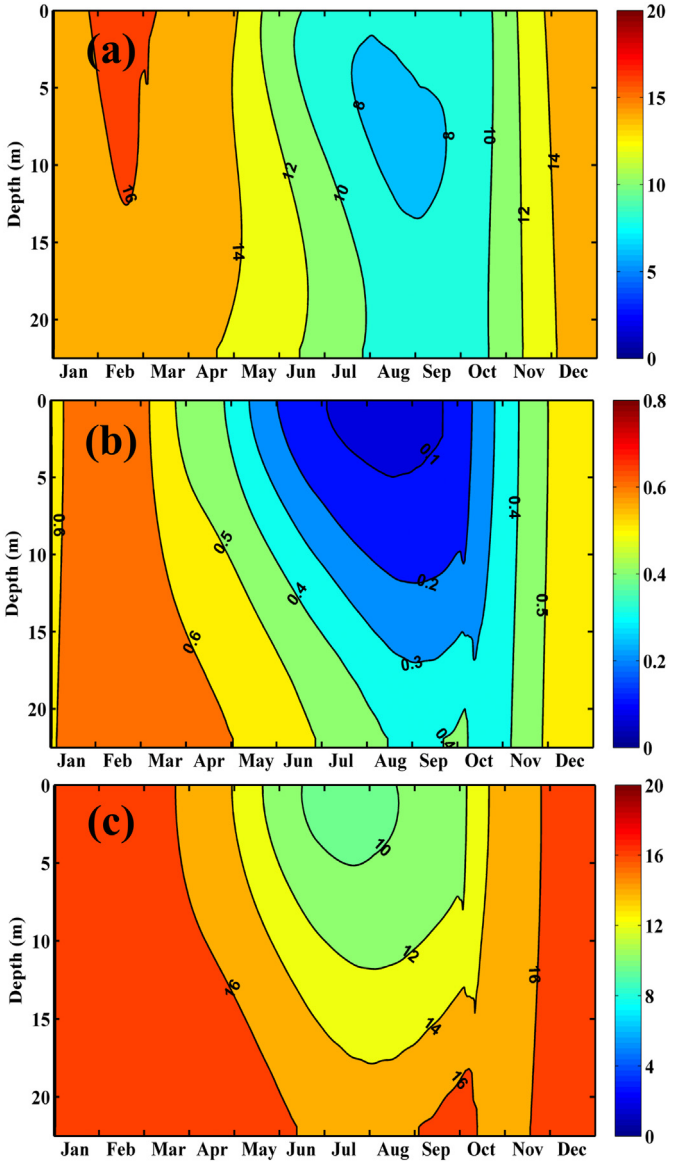

Fig. 3. Monthly concentrations of DIN (a), DIP (b), and DSi (c) at different depths. Unit: mmol m^{-3}.

3.2. Seasonal variations of particulate concentration

Although this study focuses on the seasonal variations in nutrients, nutrient cycling is closely related to changes in particulate materials such as plankton and detritus. Here, we present the modeled seasonal variations in these particulate materials. As shown in Fig. S4, chlorophyll-a (Chl-a), an index of phytoplankton biomass, exhibited an apparent seasonal variation in the CBS, which was consistent with the observational data. The vertical mean Chl-a concentrations in winter, spring, summer, and autumn were 0.56 mg m^{-3}, 1.1 mg m^{-3}, 2.0 mg m^{-3}, and 1.0 mg m^{-3}, respectively. The Chl-a concentrations were slightly higher in surface water than in bottom water in spring and summer, whereas they exhibited a vertically homogenous distribution in autumn and winter.

The particulate materials peaked in summer with the highest concentration of ~1.2 mmol N m^{-3} for phytoplankton, ~1.8 mmol N m^{-3} for zooplankton, ~6.0 mmol N m^{-3} for PON, ~0.3 mmol P m^{-3} for POP, and ~6.0 mmol Si m^{-3} for BSi (Fig. S5). Although these particulate materials exhibited higher concentrations in surface water than in bottom

water in summer, there was no obvious vertical difference between them in other seasons. In addition, the peak zooplankton concentration occurred approximately one month after that of phytoplankton (Fig. S5a, b). In summer, the increase in phytoplankton biomass provides a more adequate source of food for zooplankton, which in turn leads to an increase in zooplankton biomass, indicating a bottom-up control in the plankton ecosystem. Compared to the limited observational data for particulate materials, our simulated values were of the same order of magnitude as those reported in recent years (Xu et al., 2016; Wang et al., 2018b; Bu et al., 2019; Zhai et al., 2019).

3.3. Nutrient budget for each season

The model simulations provided a budget for all compartments in the CBS (Fig. 4). The sources and sinks of nutrients include river input, atmospheric nitrogen deposition, sediment release, benthic nitrogen loss, phytoplankton uptake and respiration, zooplankton excretion, and organic matter mineralization. For DIN, benthic nitrogen loss (0.4–0.6 mmol m^{-2} d^{-1}) was comparable to, but greater than, each external input (river input, 0.1–0.4 mmol m^{-2} d^{-1}; atmospheric deposition, 0.2–0.4 mmol m^{-2} d^{-1}; sediment release, 0.1–0.4 mmol m^{-2} d^{-1}). River inputs of DIP (0.6–4.4 μmol m^{-2} d^{-1}) and DSi (0.1–0.2 mmol m^{-2} d^{-1}) were slightly lower than their respective sediment release fluxes (DIP: 5–16 μmol m^{-2} d^{-1}; DSi: 0.1–0.5 mmol m^{-2} d^{-1}). It was noteworthy that the above external nutrient fluxes were considerably lower than those due to biological processes (e.g., summer values of 3.2–14.5 mmol m^{-2} d^{-1} for DIN, 163–732 μmol m^{-2} d^{-1} for DIP, and 1.9–7.8 mmol m^{-2} d^{-1} for DSi). Phytoplankton uptake was the largest sink for nutrients in seawater, with the highest values in summer (DIN: 14.5 mmol m^{-2} d^{-1}; DIP: 0.73 mmol m^{-2} d^{-1}; DSi: 7.8 mmol m^{-2} d^{-1}). The other biological processes (phytoplankton respiration, zooplankton excretion, and organic matter mineralization) replenished the nutrients used by photosynthesis.

Based on the nutrient inventory and fluxes of different processes in seawater, we calculated the conversion time (γ) of nutrients using Eq. (5) for the different processes. The γ values of phytoplankton uptake for DIN, DIP, and DSi were approximately 13 d, 6 d, and 36 d in summer, and 321 d, 171 d, and 481 d in winter. As the nutrient inventory in winter was only 1–3 times higher than that in summer (Fig. 4), the large variation in γ of phytoplankton uptake likely depended on the nutrient uptake flux, whose seasonal variation would have led to rapid nutrient cycling in summer.

3.4. Seasonal variations of nutrient ratios

As a result of the seasonal variations in nutrient concentrations, the nutrient molecular ratios also exhibited significant seasonal variations in the CBS (Fig. 5a). The N/P ratio was obviously higher in summer in comparison with that in other seasons. The summertime N/P ratio exhibited an obviously vertical difference with a higher value in surface water (~100) than in bottom water (<30). However, there was almost no vertical variation in the N/P ratio in winter, which was <30. The Si/N ratio also presented some seasonal variations that were not as significant as those of the N/P ratio (Fig. 5b). The Si/N ratio was slightly higher in summer than in other seasons, with the highest value of ~1.8 in bottom water. The Si/N ratio was vertically homogeneous in winter, with a value of ~1. The slight seasonal variation in the Si/N ratio was mainly caused by the competition between diatoms and dinoflagellates (see Text S5 in detail).

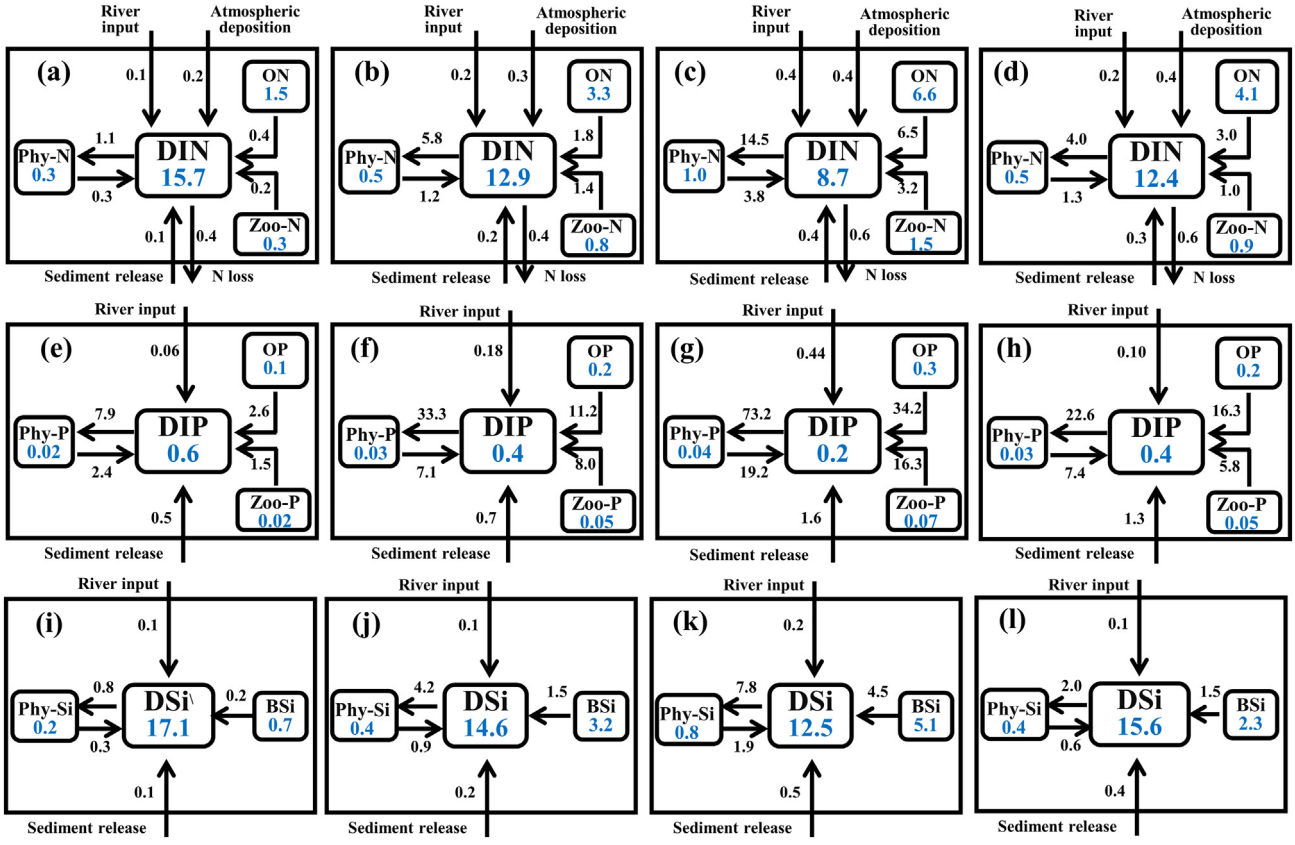

Fig. 4. Seasonal budgets for nutrients in the central Bohai Sea. The blue numbers are the vertical mean concentrations (mmol/m^3) of variables, including phytoplankton nitrogen content (Phy-N), phytoplankton phosphorus content (Phy-P), phytoplankton silicon content (Phy-Si), zooplankton nitrogen content (Zoo-N), zooplankton phosphorus content (Zoo-P), zooplankton silicon content (Zoo-Si), dissolved inorganic nitrogen (DIN), dissolved inorganic phosphorus (DIP), dissolved silicate (DSi), organic nitrogen (ON), organic phosphorus (OP), and biogenic silica (BSi). The black numbers denote the vertically integrated nutrients fluxes (DIN and DSi: mmol m^{-2} d^{-1}; DIP: 10^{-2} mmol m^{-2} d^{-1}). (a, e, i) winter; (b, f, j) spring; (c, g, k) summer; (d, h, l) autumn. (For interpretation of the references to color in this figure legend, the reader is referred to the web version of this article.)

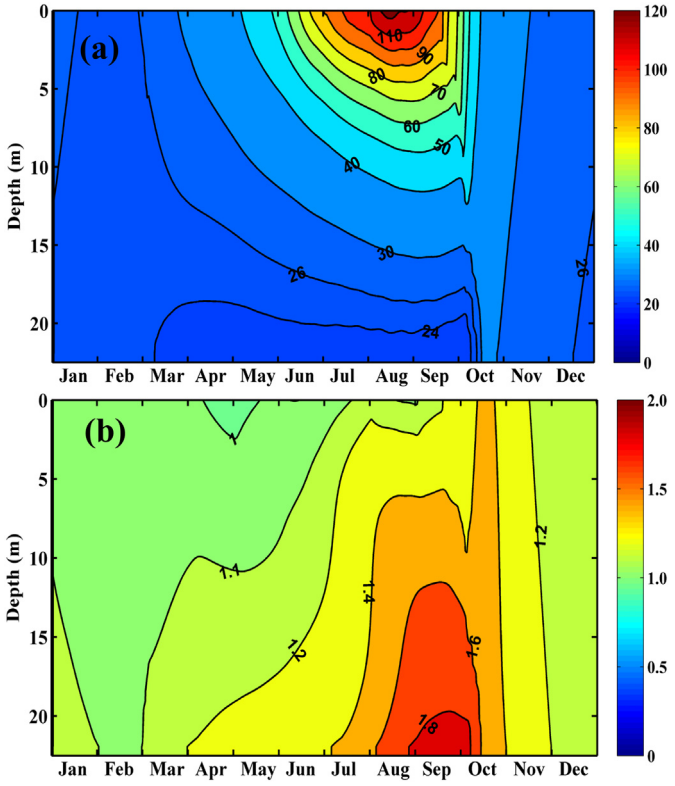

Fig. 5. Monthly N/P ratio (a) and Si/N ratio (b) at different depths.

4. Discussion

4.1. Effects of multiple processes on seasonal variations of nutrients

Many studies have found that the nutrients in the Bohai Sea were supplied by riverine inputs (Liu et al., 2009), atmospheric deposition (Shou et al., 2018; Qi et al., 2020), and sediment release (Liu et al., 2011). Benthic nitrogen loss at the water–sediment interface played an important role in removing nitrogen from seawater (Zhang et al., 2018; Zheng et al., 2020). Seasonal differences in the above processes at their boundaries naturally affect the seasonal variations of nutrient concentrations in seawater. Moreover, nutrient budgets have indicated the important role of biological processes in promoting the rapid conversion of nutrients in seawater, especially in summer (Fig. 4). Therefore, we designed a series of numerical experiments to examine the effects of these processes on the seasonal variations of nutrient in the CBS (see Section 2.4 for details of the configuration).

Fig. 6 showed the vertical mean values of the simulated DIN, DIP, and N/P ratio of seawater in different numerical experiments. The seasonal variations of DIN, DIP, and the N/P ratio in the control group (Case 0) changed completely when biological processes were excluded in Case 1, indicating the critical role of biological processes in the seasonal variations of nutrients in the CBS. In comparison to Case 0 (after one year of integration), the simulated DIN concentration in Case 2 (river input excluded), Case 3 (atmospheric deposition excluded), and Case 4 (sediment nutrient release excluded) decreased by 3 mmol m^{-3}, 4 mmol m^{-3}, and 3 mmol m^{-3}, respectively, while those for DIP decreased by 0.05 mmol m^{-3}, 0 mmol m^{-3}, and 0.16 mmol m^{-3}, respectively. Because of the different N/P ratios in external inputs compared to seawater, the vertical mean value of the N/P ratio decreased by ~6 in Case 2 and ~10 in Case 3, but increased by ~3 in Case 4, in comparison to Case 0 in summer. When benthic nitrogen loss was excluded (Case 5), the DIN concentration increased by 9.1 mmol m^{-3} after one year of integration compared with Case 0, which increased the N/P ratio by ~12. Overall, the comparison of results in different numerical

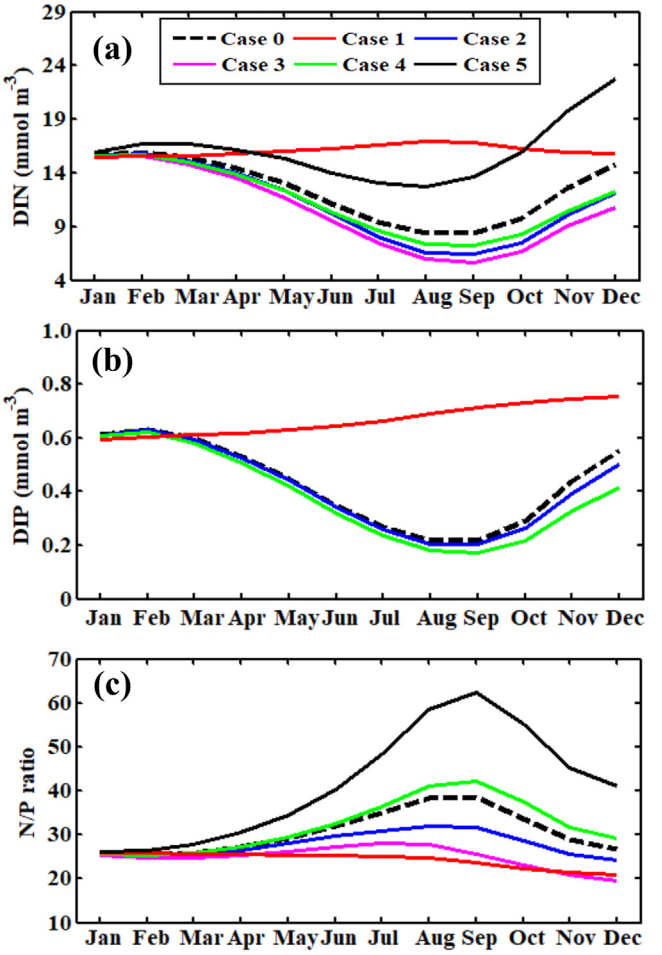

Fig. 6. Mean monthly vertical DIN (a), DIP (b), and N/P ratio (c) in different numerical experiments. In subfigure (b), the line of Case 0 overlaps the lines of Case 3 and Case 5.

experiments exhibited that biological processes played the most important role in the seasonal variation of nutrients, although the other processes such as external input and output could also affect the concentration of nutrients. It must be noted that although the physical factors such as light intensity and water temperature have no direct effects on the nutrient budget, they actually affects the biological processes.

As described in Section 2.4, we defined five variables to evaluate the contribution of each process to the seasonal variation: (1) ΔNF_i^j and (2) ΔPF_i^j to determine the change in the DIN and DIP fluxes between Case 0 and Cases 1–5; (3) RN_i^j, (4) RP_i^j, and (5) RNP_i^j to determine the percentages of the DIN concentration, DIP concentration, and N/P ratio in Case 0 changed by the process excluded in the other five cases.

4.1.1. Biological processes

Fig. 7a and b indicated that biological processes led to the highest nutrient removal rates (DIN: 1.9 mmol m^{-2} d^{-1}; DIP: 0.08 mmol m^{-2} d^{-1}) in summer, while they replenished a large fraction of nutrients in autumn. The inclusion of biological processes also resulted in a slight increase of sediment release (DIN: <0.3 mmol m^{-2} d^{-1}; DIP: <0.01 mmol m^{-2} d^{-1}) and a decrease of benthic nitrogen loss (DIN: <0.4 mmol m^{-2} d^{-1}) during summer and autumn. Fig. 8a and b showed that the DIN and DIP concentrations in Case 0 increased by ~100% and ~200% in summer when biological processes were excluded in Case 1. Because of the difference in each flux (Fig. 7a–b), the increases in DIN and DIP in summer in Case 1 relative to Case 0 were mainly induced by the direct effect of biological processes within seawater rather than

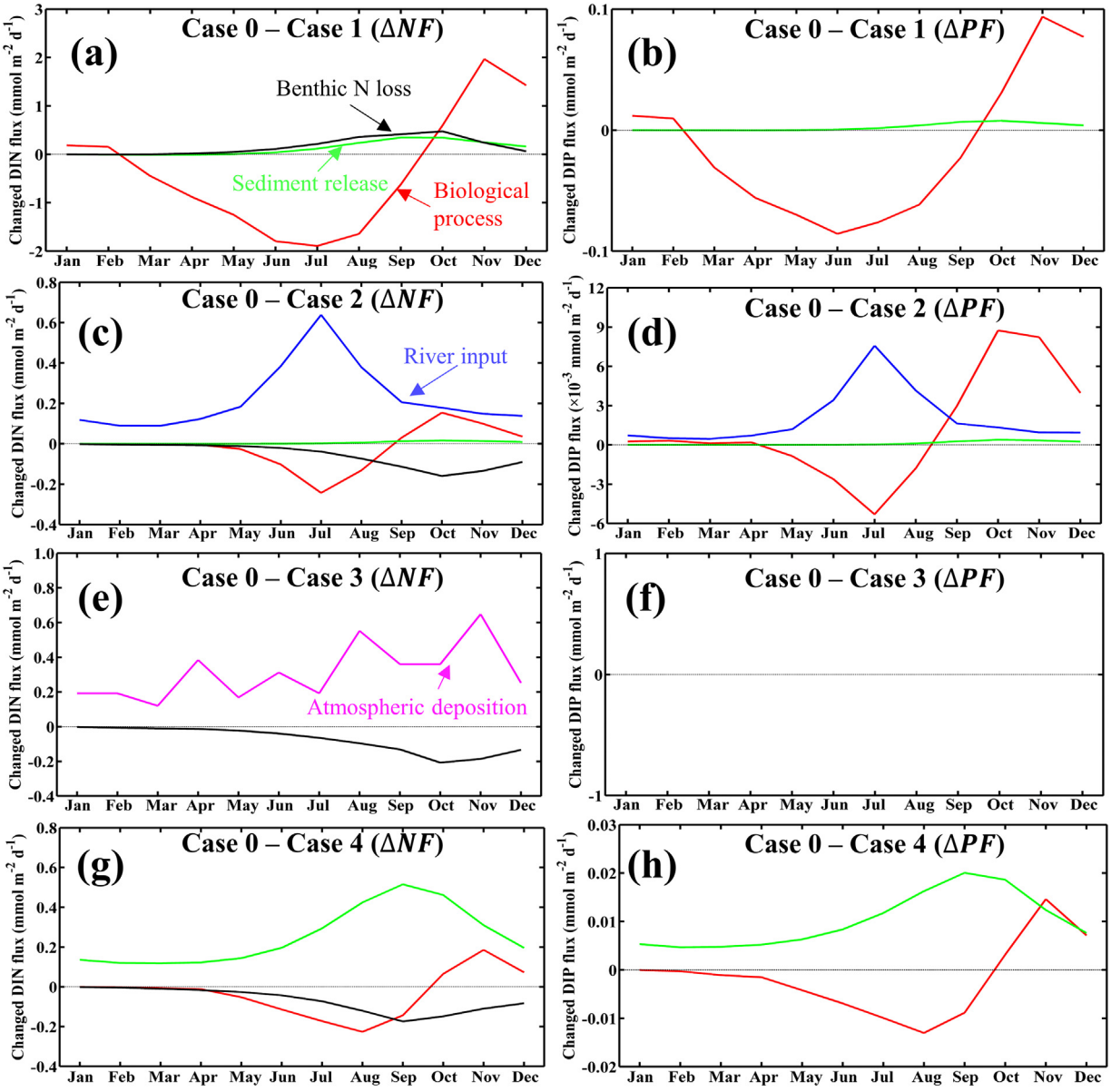

Fig. 7. Changed fluxes of various nutrient-related processes for DIN (a, c, e, g) and DIP (b, d, f, h) using the results of Case 0 minus those in the numerical experiments (Cases 1 to 4). The colored solid lines represent different processes corresponding to the words shown in the same color. Positive values correspond to increasing nutrient concentrations after adding the process (see Eq. (2) for calculating Δ*NF* and Δ*PF*). (For interpretation of the references to color in this figure legend, the reader is referred to the web version of this article.)

by changes in the release of nutrients from sediment and/or benthic nitrogen loss.

Because of the lower N/P ratio involved in biological processes compared with ambient seawater, the N/P ratio of seawater in Case 0 decreased by ~25% in summer when the direct effect of biological processes was excluded (Fig. 8c). Although this had little effect on the nutrient concentrations, the changes in release of nutrients from sediments and benthic nitrogen loss in Case 1 led to decreases of ~5% and ~20% in the seawater N/P ratio in Case 0 during summer and autumn (Fig. 8c). These reductions related to the lower N/P ratio associated with sediment release and the higher N/P ratio associated with benthic nitrogen loss compared with seawater. Therefore, the seawater N/P ratio of Case 0 reduced by >40% during summer when biological processes were excluded (Fig. 8c).

The Bohai Sea is an important fishing ground in China, and its maximum primary productivity can reach 1500 mg C m^{-2} d^{-1} in summer (COOA, 2016). Strong phytoplankton photosynthesis in summer (Ding et al., 2020) results in low nutrient concentrations in seawater following their uptake. Cultivation experiments revealed that the N/P ratio in phytoplankton uptake (3–160) was always lower than the seawater N/P ratio (4–330) under different nutrient levels in the Bohai Sea (Zou et al., 2001). Consequently, the seawater N/P ratio increased significantly with enhanced phytoplankton photosynthesis in summer. In addition, most of the organic matter sequestered in marine sediments comes from the deposition of organic matter biosynthesized by marine organisms inhabiting surface waters (Wakeham and Lee, 1993). Although the organic matter in sediment could be mineralized into inorganic nutrients and then returned to the upper water column, a time lag of the order of several months exists between the deposition of particulate material and its mineralization in sediment (Rudnick and Oviatt, 1986). This was demonstrated by the increased nutrient release from sediment after strong biological processes in summer in the present study (Fig. 7a, b). Strong biological processes in summer also reduced the flux of benthic nitrogen loss (Fig. 7a) by absorbing DIN, which is an important substrate for benthic nitrogen loss (Fennel, 2017).

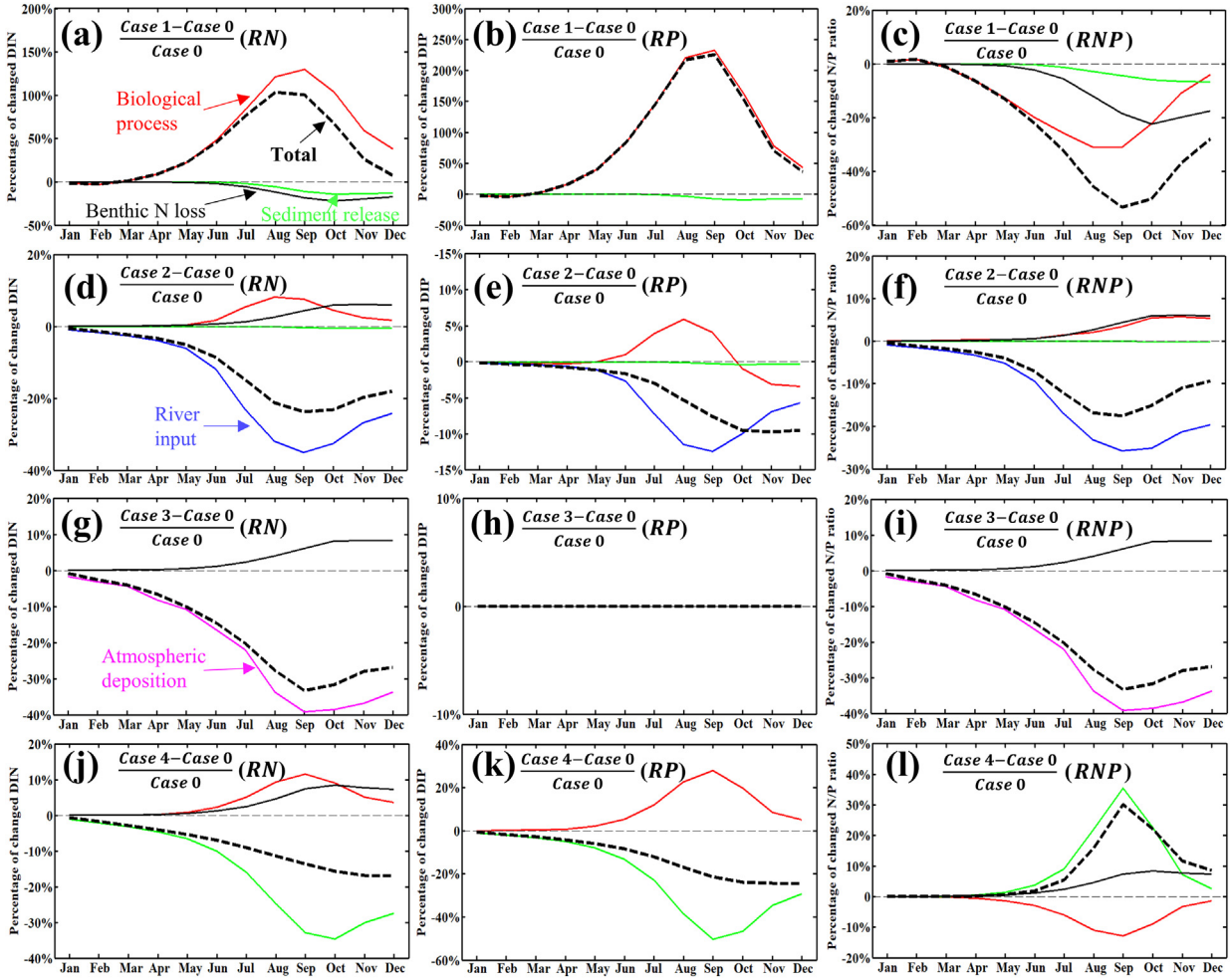

Fig. 8. Changed percentages of DIN (a, d, g, j), DIP (b, e, h, k), and the N/P ratio (c, f, i, l) due to the changed processes in the numerical experiments (Cases 1 to 4) relative to the results of the control group (Case 0). The colored lines represent different processes corresponding to the words shown in the same color. Positive values correspond to increasing nutrient concentrations or the N/P ratio in Case 0 if excluding the process (see Eqs. (3) and (4) for calculating *RN*, *RP*, and *RNP*). (For interpretation of the references to color in this figure legend, the reader is referred to the web version of this article.)

4.1.2. River input

As shown in Fig. 7c and d, river inputs supplied a large amount of nutrients to the CBS, with the highest fluxes of ~0.6 mmol m^{-2} d^{-1} for DIN and ~0.008 mmol m^{-2} d^{-1} for DIP in summer. These riverine nutrient fluxes resulted in a higher nutrient consumption by biological processes in summer (DIN: ~0.2 mmol m^{-2} d^{-1}; DIP: ~0.002 mmol m^{-2} d^{-1}). The additional organic matter in summer replenished nutrients through remineralization in autumn. Moreover, benthic nitrogen loss also increased after summer because the bottom DIN concentration increased, with the highest value of ~0.18 mmol m^{-2} d^{-1} (Fig. 7c). A slightly increased nutrient flux from sediment release was also confirmed in autumn when river input was included in the simulation (Fig. 7c, d). Fig. 8d and e showed that the DIN concentration, DIP concentration, and N/P ratio in Case 0 decreased by >30%, >10%, and >20% in summer when the direct effect of river input was excluded. The changes in the effects of biological processes, benthic nitrogen loss, and sediment nutrient release on the nutrient concentrations and N/P ratio were limited to <10% when river input was included in the simulation (Fig. 8d–f).

Although many studies have emphasized the importance of riverine inputs in supplying seawater nutrients in summer in the coastal waters of the Bohai Sea (Wang et al., 2017), the nutrient fluxes of river input were still much lower than the nutrient loss in biological processes (Fig. 4). Consequently, the river inputs cannot replenish the loss of nutrients due to the strong biological processes in summer. This leads to the occurrence of the lowest nutrient concentrations in summer in the CBS. Nevertheless, as the N/P ratio of river water (>300) is much higher than that of seawater (Liu et al., 2012), the large amount of nutrients transported by river discharge into the sea led to an increase in the seawater N/P ratio (Fig. 6).

4.1.3. Atmospheric deposition

Fig. 7e showed that the DIN flux of atmospheric deposition was slightly higher in summer and autumn (0.2–0.6 mmol m^{-2} d^{-1}) than in winter and spring (0.1–0.4 mmol m^{-2} d^{-1}). With the inclusion of atmospheric deposition, the benthic nitrogen loss increased by ~0.2 mmol m^{-2} d^{-1} for DIN after summer (Fig. 7e). Atmospheric deposition of DIN did not affect biological processes because the limiting nutrient in the CBS is phosphate (Wang et al., 2009; Xu et al., 2011), which was not provided via atmospheric deposition. Fig. 8g and i reveal that both the DIN and N/P ratio in Case 0 decrease by >30% in summer when the direct effect of atmospheric deposition was excluded. The change in the benthic nitrogen loss caused by atmospheric deposition led to a <12% increase in both the DIN concentration and N/P ratio in Case 0 (Fig. 8g, i). The DIN flux of atmospheric deposition was comparable to that of river inputs into the CBS (Fig. 4), which has been emphasized in recent studies (Shou et al., 2018; J.J. Wang et al., 2019; Zhang et al., 2020). However, the limiting nutrient for phytoplankton growth in the Bohai Sea has changed to phosphorus owing to excessive nitrogen input (Wang et al., 2009; Xu et al., 2011). Thus, it is necessary to rethink the role of atmospheric deposition in primary production because the previous

calculation based on the atmospheric deposition of nitrogen is likely an overestimation.

4.1.4. Sediment nutrient release

Our simulated nutrient fluxes (NH_4^+: <0.6 mmol m^{-2} d^{-1}; DIP: <0.02 mmol m^{-2} d^{-1}) released from sediments in the CBS were consistent with the observational data (see Text S4 for details). Fig. 7g and h showed that the nutrient flux from sediment was higher in summer and autumn than in winter and spring. Because of the large amount of organic matter accumulated in the summer (Fig. S5) and the highest bottom water temperature in September (Fig. S8), the mineralization rate of organic matter in sediment was highest in September, which led to the highest sediment nutrient flux. The DIN and DOP removed by biological processes increased by ~0.2 mmol m^{-2} d^{-1} and ~0.01 mmol m^{-2} d^{-1}, respectively, in summer due to sediment release (Fig. 7g, h). These nutrients were replenished in autumn by the mineralization of organic matter. In addition, the DIN flux associated with benthic nitrogen loss increased by <0.2 mmol m^{-2} d^{-1} when sediment nutrient release was included in the simulation (Fig. 7g). Fig. 8j and k showed that the DIN and DIP concentrations in Case 0 decreased by ~30% and ~45%, respectively, in summer and autumn when the direct effect of sediment nutrient release was excluded. The change in biological processes caused by sediment nutrient release led to a ~7% increase in DIN and ~25% increase in DIP in summer with respect to Case 0, while the change in benthic nitrogen loss led to a <8% increase in DIN in summer and autumn. Because the N/P ratio in the sediment was lower than that in seawater, the seawater N/P ratio of Case 0 increased by >20% in summer when sediment nutrient release was excluded (Fig. 8l). The N/P ratio of Case 0 for summer and autumn decreased by <10% due to biological processes and increased by <7% due to benthic nitrogen loss when sediment nutrient release was excluded. Overall, sediment release is an important source of nutrients in the Bohai Sea (Liu et al., 2011; Mu et al., 2017), and hinders the decrease in nutrient concentrations while increasing the N/P ratio in summer.

4.1.5. Importance of benthic nitrogen loss

Benthic nitrogen loss via denitrification and anaerobic ammonium oxidation plays a critical role in removing nitrogen from coastal waters (Fennel, 2017). The limited observational data indicate that nitrogen loss at the sediment–water interface is an important sink of DIN in the Bohai Sea (Zhang et al., 2018; Zheng et al., 2020). However, the specific regulatory mechanisms of benthic nitrogen loss have large uncertainties. In this study, we represented the benthic nitrogen loss rate as a function of the bottom temperature and nitrate concentration (Eq. (S69)), according to Yoshikawa et al., 2005 and Tan et al. (2020). The calculated annually averaged flux of benthic nitrogen loss was 0.49 mmol m^{-2} d^{-1}, which is close to an observed value of 0.37 mmol m^{-2} d^{-1} (Zhang et al., 2018; Zheng et al., 2020). The fluxes of benthic nitrogen loss in each season exceeded 50% of the DIN inputs from rivers and the atmosphere in the CBS (Fig. 4a–d). Fig. 6a indicated that the DIN concentration decreased by >5 mmol m^{-3} in summer when benthic nitrogen loss was included in the simulation. Consequently, the increase in the N/P ratio in seawater was greatly suppressed by the benthic nitrogen loss, which prevented the seawater N/P ratio from rising by >20 in summer (Fig. 6c). Overall, benthic nitrogen loss is of great importance to the seasonal variations of the DIN concentration and N/P ratio in the CBS, and is second to the influence of biological process.

In this study, we also examined the extent to which the calculated DIN concentration varied with the rate of benthic nitrogen loss (n_0 in Eq. (S69)). For this purpose, we increased and decreased the value of n_0 by 50% and ran the model for a year in each of the sensitivity experiments. The sensitivity of the DIN concentration to n_0 was quantified by a factor of $S = |\frac{\Delta C/C}{\Delta\alpha/\alpha}|$ (Pan et al., 2017), where C is the annual mean DIN concentration, α is the value of n_0 used in the model, and ΔC is the variation in C corresponding to the change ($\Delta\alpha$) of the parameter n_0. The results of sensitivity experiments suggested an S value of 0.21, indicating that the DIN concentration in our model was not very sensitive to the value of n_0. Thus, the benthic nitrogen loss given by the model can be considered a robust estimation.

Field observational data and experimental data indicate that some environmental factors, such as the bottom oxygen concentration, the quantity and quality of organic matter, and microbial functional traits, may also affect the rate of benthic nitrogen loss (Zhang et al., 2018; Song et al., 2020). However, little is known about the specific functional relationship between the removal rate and these environmental factors (Fennel, 2017). With a better understanding of these relationships in the future, a more comprehensive model of benthic nitrogen loss is expected.

Fig. 9 summarized the summertime effects of the interactions among nutrient-related processes on the nutrient concentrations and N/P ratio in the CBS. Overall, biological processes play a critical role in decreasing the nutrient concentrations and increasing the N/P ratio through the direct effect of phytoplankton uptake. The external inputs of nutrients through boundaries such as river input, atmospheric deposition, and sediment release are important sources of nutrients in seawater, which can also affect nutrient concentrations and N/P ratio by affecting other nutrient-related processes. Benthic nitrogen loss is essential for maintaining the nitrogen balance in the sea by directly removing a large amount of inorganic nitrogen.

4.2. Effect of nitrogen-to-phosphorus stoichiometry in phytoplankton uptake

The Redfield ratio (N:P = 16:1) is widely used to link marine nitrogen and phosphorus cycles in many biogeochemical models (Anderson and Sarmiento, 1994; Laurent et al., 2012). However, empirical and theoretical studies have shown that the ratio of nitrogen to phosphorus in phytoplankton uptake varies with growth conditions (Mills and Arrigo, 2010; Garcia et al., 2018). In the Bohai Sea, incubation experiments have also shown that the N/P ratio of phytoplankton uptake depends on the nutrient ratio in ambient seawater (Zou et al., 2001). Therefore, the use of a fixed ratio in modelling biogeochemical processes in the CBS is not a good choice.

Galbraith and Martiny (2015) found that the N/P ratio in plankton changed largely across the typical range of DIP concentrations in the ocean, while it changes only slightly at very low DIN concentrations. Accordingly, Macias et al. (2019) provided a parameterized solution describing the variation in the N/P ratio of phytoplankton uptake as a function of the DIP concentration in seawater (Eq. (S26)), which had been applied in biogeochemical simulations of marginal seas with excessive nitrogen. In this study, we used the scheme provided by Macias et al. (2019) to include the variation of the N/P ratio in phytoplankton uptake.

To estimate the effect of the variation of the N/P ratio in phytoplankton uptake on the seasonal variation of nutrient concentrations, we conducted another numerical experiment (Case 6) in which the N/P ratio in phytoplankton uptake followed the fixed Redfield stoichiometry.

As shown in Fig. S9a–c, the DIN concentration decreased obviously from June to October in Case 0 compared with Case 6, with the highest reduction of >2.5 mmol m^{-3} in surface water. There was no difference in the DIP concentration between the two cases (Fig. S9d–f). The Bohai Sea experiences serious phosphorous limitation, with an N/P ratio much higher than 16, especially in summer (Wang et al., 2009; Xu et al., 2011). The low DIP concentration led to a stable DIP flux of phytoplankton uptake in the two cases. Because the N/P ratio in phytoplankton uptake increased in summer due to the decreased DIP concentration in Case 0, more DIN was removed in Case 0 than in Case 6. Consequently, the N/P ratio of seawater decreased more (>18) in Case 0 than in Case 6 in summer (Fig. S9g–i). In cold months, the relatively high DIP concentration allowed the N/P ratio of phytoplankton uptake similar to the

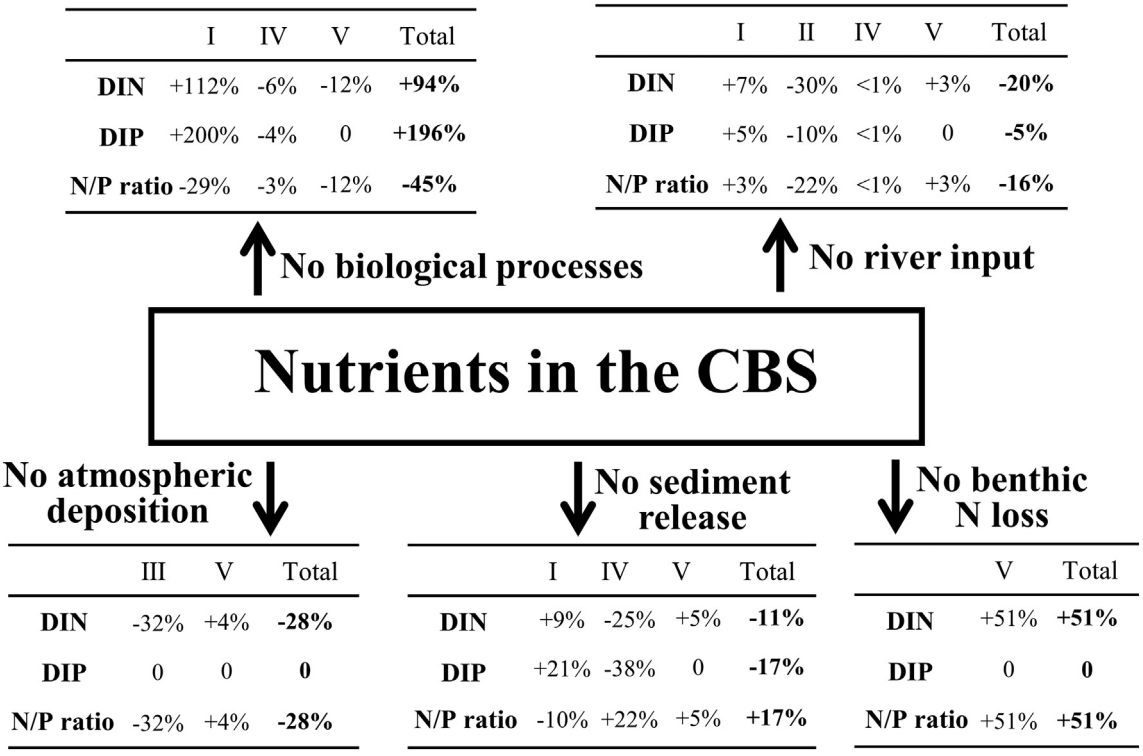

Fig. 9. Changed percentages of DIN, DIP, and the N/P ratio in summer due to the interactions among nutrient-related processes if one specific factor is excluded. I, II, III, IV, and V represent biological processes, river input, atmospheric deposition, sediment release, and benthic nitrogen loss, respectively.

Redfield ratio. Consequently, the DIN concentration and N/P ratio in seawater were almost the same in the two cases in cold months.

4.3. Implications for seasonal variations of nutrients in global coastal waters

To deepen our understanding of the seasonal variation of nutrients in coastal waters, we present a comparison of our results in the CBS with the reported results in other coastal waters worldwide. As shown in Table 2, the nutrient concentrations in the CBS varied within the range of those reported for other coastal waters. Similar to the CBS, nutrient concentrations and the N/P ratio also exhibited significant seasonal variations in other coastal waters. However, there are many control mechanisms for the seasonal variation of nutrients in various coastal waters. For example, phytoplankton growth is the dominant factor modifying the seasonal variation of nutrients in the Baltic Sea, Black Sea, and Seto Inland Sea, which is similar to the results for the CBS. Terrestrial inputs play a critical role in the seasonal variation of nutrients in the Yangtze River Estuary, northern Beibu Gulf, and Chesapeake Bay. Anthropogenic runoff increases nutrient concentrations during the northeast monsoon in the Bay of Bengal. The transportation of nutrients by seasonal ocean currents leads to a significant seasonal variation of nutrients in the coastal waters of Namibia and the northern Galician coast. The seasonal variation of nutrients in the coastal Yellow Sea and

Table 2
Comparison of the seasonal variations in nutrient concentrations of coastal waters worldwide.

Area	Nutrient concentration (mmol m^{-3})				N/P ratio		Dominant factor	References
	DIN	DIP	DSi	Seasonal variation	Value	Seasonal variation		
Central Bohai Sea	6–18	0–0.8	8–18	Lowest in summer	20–120	Peak in summer	Biological processes	[1]
Coastal Yellow Sea	4.5–15	0.1–0.6	3–12	Lowest in March, May, and June	23–77	Highest in spring	Terrestrial input and phytoplankton growth	[2]
Yangtze River Estuary	0–40	0–1	0–80	Highest in summer	10–400	Highest in summer	River input	[3]
Northern Beibu Gulf	0–65	0–2.5	0–112	Peak in summer	10–40	Peak in summer	River input	[4]
Bay of Bengal	0–21	0–7	6–28	Peak during the northeast monsoon	0.5–84	Peak in December	Anthropogenic runoff	[5]
Baltic Sea	0.4–21	0–1.1	2–26	Lowest in summer	5–132	Lowest in summer	Phytoplankton growth	[6,7]
Black Sea	0–3	–	0–3	Lowest in summer	–	–	Phytoplankton growth	[8]
Eastern Seto Inland Sea	0.5–8	0.1–0.9	1–30	Lowest in spring–summer	0–10	Highest in spring–summer	Phytoplankton growth	[9]
Chesapeake Bay	0–125	0.1–1.3	0–100	Highest DIN and DSi in winter–spring; highest DIP in summer	1–1000	Highest in winter–spring	Terrestrial input	[10]
Eastern Gulf of Mexico (Florida Bay)	0–40	0–0.2	–	Lowest DIN in summer; no obvious seasonality for DIP	15–500	Lowest in summer	Water exchange and phytoplankton growth	[11]
Coastal waters off Namibia	4–30	–	0–40	Peak in spring	–	–	Benguela upwelling	[12]
Northern Galician coast	0.5–10	0.1–0.8	0–4	Highest in summer	3–18	Highest in summer	Coastal upwelling	[13]

[1] This study; [2] Shi et al. (2015); [3] Fan and Song (2014); [4] Lai et al. (2014); [5] Achary et al. (2014); [6] Lyngsgaard et al. (2017); [7] Purina et al. (2018); [8] Grégoire et al. (2008); [9] Yamaguchi et al. (2020); [10] Malone et al. (1996); [11] Pennock et al. (1999); [12] Louw et al. (2016); [13] Caseas et al. (1997).

Florida Bay is caused by several factors (Table 2). Overall, our quantitative analysis of the effects of multiple processes on seasonal variations of nutrient in the CBS provides an important reference for similar studies in other coastal waters.

5. Summary

In this study, a physical–biological coupled model was developed to analyze the impact of external nutrient inputs and biological processes on the seasonal variations of nutrients in the CBS. The model results showed significant seasonal variations in nutrient concentrations and the N/P ratio. In summer, a large amount of nutrients was consumed during phytoplankton photosynthesis, in which the nitrogen-to-phosphorus stoichiometry in phytoplankton uptake was lower than the N/P ratio of seawater. This process was the major cause of the lowest nutrient concentrations and the highest N/P ratio in summer. River inputs, atmospheric deposition, and sediment nutrient release replenished nutrients, which, to some extent, alleviated the decrease in nutrient concentrations in summer. Benthic nitrogen loss was essential for maintaining the nitrogen balance in the CBS by removing a large amount of inorganic nitrogen in summer and autumn. Additionally, we demonstrated that the variation in nitrogen-to-phosphorus stoichiometry of phytoplankton uptake with the N/P ratio of ambient seawater is also an important factor affecting the nutrient ratio in the CBS. Therefore, such variation should be included in future studies to obtain a better understanding of the nutrient dynamics in coastal waters. This work is a reference for establishing water quality management plans aimed at mitigating the negative impacts of nutrient pollution (i.e., eutrophication) in global coastal seas.

CRediT authorship contribution statement

Xiaokun Ding: Writing – original draft. **Xinyu Guo:** Writing – review & editing. **Huiwang Gao:** Writing – review & editing. **Jie Gao:** Data curation. **Jie Shi:** Methodology. **Xiaojie Yu:** Resources. **Zhaosen Wu:** Software.

Declaration of competing interest

The authors whose names are listed immediately below certify that they have no affiliations with or involvement in any organization or entity with any financial interest (such as honoraria; educational grants; participation in speakers' bureaus; membership, employment, consultancies, stock ownership, or other equity interest; and expert testimony or patent-licensing arrangements), or non-financial interest (such as personal or professional relationships, affiliations, knowledge or beliefs) in the subject matter or materials discussed in this manuscript.

Acknowledgements

This study is funded by the National Natural Science Foundation of China-Shandong Joint Fund for Marine Science Research Centers (U1906215, U1806211) and NSFC (41876125). X. Ding thanks the China Scholarship Council (CSC) for supporting his stay in Japan and the Ministry of Education, Culture, Sports, Science and Technology, Japan (MEXT) to a project on Joint Usage/Research Center, Leading Academia in Marine and Environmental Research (LaMer) for supporting his study in Japan. We also thank Dr. Naoki Yoshie for providing the source code of NEMURO.

Appendix A. Supplementary data

Supplementary data to this article can be found online at https://doi.org/10.1016/j.scitotenv.2021.149416.

References

Achary, M.S., Panigrahi, S., Satpathy, K.K., Sahu, G., Mohanty, A.K., Selvanayagam, M., Panigrahy, R.C., 2014. Nutrient dynamics and seasonal variation of phytoplankton assemblages in the coastal waters of southwest bay of Bengal. Environ. Monit. Assess. 186 (9), 5681–5695.

Anderson, L.A., Sarmiento, J.L., 1994. Redfield ratios of remineralization determined by nutrient data analysis. Glob. Biogeochem. Cycles 8 (1), 65–80.

Blumberg, A.F., Mellor, G.L., 1987. A description of a three-dimensional coastal ocean circulation model. In: Heaps, N.S. (Ed.), Three-Dimensional Coastal Ocean Models. AGU, Washington, D. C, pp. 1–16.

Bristow, L.A., Mohr, W., Ahmerkamp, S., Kuypers, M.M.M., 2017. Nutrients that limit growth in the ocean. Curr. Biol. 27 (11), R474–R478.

Bu, Y.Q., Zhu, L.Y., Cheng, X., Dong, H.H., Sui, Y., Wang, C., 2019. Community structure of zooplankton and its relationship with environmental factors in the Bohai and the north Huanghai Sea in summer and winter. Period. Ocean Univ. China 49 (02), 59–66 (In Chinese with English abstract).

Capet, A., Meysman, F.J.R., Akoumianaki, I., Soetaert, K., Grégoire, M., 2016. Integrating sediment biogeochemistry into 3D oceanic models: a study of benthic-pelagic coupling in the Black Sea. Ocean Model 101, 83–100.

Caseas, B., Varela, M., Canle, N., Gonzalez, N., Bode, A., 1997. Seasonal variations of nutrients, seston and phytoplankton, and upwelling intensity off La coruna (NW Spain). Estuar. Coast. Shelf Sci. 6 (44), 767–778.

Chen, Y., Gao, Y., Chen, C., Liang, J., Sun, L., Zhen, Y., Qiao, L., 2016. Seasonal variations of phytoplankton assemblages and its relation to environmental variables in a scallop culture sea area of Bohai Bay China. Mar. Pollut. Bull. 113 (1–2), 362–370.

COOA, 2016. China Offshore Ocean Atlas—Marine Life and Ecology. Ocean Press, Beijing, China (In Chinese).

Ding, X.K., Guo, X.Y., Zhang, C., Yao, X.H., Liu, S.M., Shi, J., Luo, C.X., Yu, X.J., Yu, Y., Gao, H.W., 2020. Water conservancy project on the Yellow River modifies the seasonal variation of chlorophyll-a in the Bohai Sea. Chemosphere 254, 126846.

Fan, W., Song, J.B., 2014. A numerical study of the seasonal variations of nutrients in the Changjiang River estuary and its adjacent sea area. Ecol. Model. 291, 69–81.

Fennel, K., 2017. Ocean hotspots of nitrogen loss. Nature 551 (7680), 305–306.

Fennel, K., Wilkin, J., Levin, J., Moisan, J., O'Reilly, J., Haidvogel, D., 2006. Nitrogen cycling in the middle Atlantic bight: results from a three-dimensional model and implications for the North Atlantic nitrogen budget. Glob. Biogeochem. Cycles 20 (3).

Fisher, T.R., Peele, E.R., Ammerman, J.W., Harding, L.W., 1992. Nutrient limitation of phytoplankton in Chesapeake Bay. Mar. Ecol. Prog. Ser. 82 (1), 51–63.

Galbraith, E.D., Martiny, A.C., 2015. A simple nutrient-dependence mechanism for predicting the stoichiometry of marine ecosystems. Proc. Natl. Acad. Sci. 112 (27), 8199–8204.

Garcia, N.S., Sexton, J., Riggins, T., Brown, J., Lomas, M.W., Martiny, A.C., 2018. High variability in cellular stoichiometry of carbon, nitrogen, and phosphorus within classes of marine eukaryotic phytoplankton under sufficient nutrient conditions. Front. Microbiol. 9, 543.

Grégoire, M., Raick, C., Soetaert, K., 2008. Numerical modeling of the Central Black Sea ecosystem functioning during the eutrophication phase. Prog. Oceanogr. 76 (3), 286–333.

Guo, W., 2019. Modelling the Effects of the Atmospheric Nitrogen Deposition on the Primary Production Process in the Southern Yellow Sea. Master thesis. Ocean University of China, Qingdao (In Chinese with English abstract).

He, H.J., Yu, Z.G., Yao, Q.Z., Chen, H.T., Mi, T.Z., 2010. The hydrological regime and particulate size control phosphorus form in the suspended solid fraction in the dammed huanghe (Yellow River). Hydrobiologia 638 (1), 203–211.

Herut, B., Almogi-Labin, A., Jannink, N., Gertman, I., 2000. The seasonal dynamics of nutrient and chlorophyll a concentrations on the SE Mediterranean shelf-slope. Oceanol. Acta 23 (7), 771–782.

Kim, T., Lee, K., Najjar, R.G., Jeong, H., Jeong, H.J., 2011. Increasing N abundance in the northwestern Pacific Ocean due to atmospheric nitrogen deposition. Science 334 (6055), 505–509.

Kishi, M.J., Kashiwai, M., Ware, D.M., Megrey, B.A., Eslinger, D.L., Werner, F.E., Noguchi-Aita, M., Azumaya, T., Fujii, M., Hashimoto, S., Huang, D., Iizumi, H., Ishida, Y., Kang, S., Kantakov, G.A., Kim, H., Komatsu, K., Navrotsky, V.V., Smith, S.L., Tadokoro, K., Tsuda, A., Yamamura, O., Yamanaka, Y., Yokouchi, K., Yoshie, N., Zhang, J., Zuenko, Y.I., Zvalinsky, V.I., 2007. NEMURO—a lower trophic level model for the North Pacific marine ecosystem. Ecol. Model. 202 (1–2), 12–25.

Lai, J.X., Jiang, F.J., Ke, K., Xu, M.B., Lei, F., Chen, B., 2014. Nutrients distribution and trophic status assessment in the northern Beibu Gulf, China. Chin. J. Oceanol. Limnol. 32 (5), 1128–1144.

Laurent, A., Fennel, K., Hu, J., Hetland, R., 2012. Simulating the effects of phosphorus limitation in the Mississippi and Atchafalaya River plumes. Biogeosciences 9 (11), 4707–4723.

Li, Y.F., Wolanski, E., Zhang, H., 2015. What processes control the net currents through shallow straits? A review with application to the Bohai Strait, China. Estuar. Coast. Shelf Sci. 158, 1–11.

Liu, S.M., 2015. Response of nutrient transports to water–sediment regulation events in the huanghe basin and its impact on the biogeochemistry of the bohai. J. Mar. Syst. 141, 59–70.

Liu, H., Yin, B.S., 2010. Numerical investigation of nutrient limitations in the Bohai Sea. Mar. Environ. Res. 70 (3–4), 308–317.

Liu, S.M., Hong, G.H., Zhang, J., Ye, X.W., Jiang, X.L., 2009. Nutrient budgets for large chinese estuaries. Biogeosciences 6 (10), 2245–2263.

Liu, S.M., Li, L.W., Zhang, Z., 2011. Inventory of nutrients in the bohai. Cont. Shelf Res. 31 (16), 1790–1797.

Liu, S.M., Li, L.W., Zhang, G.L., Liu, Z., Yu, Z., Ren, J.L., 2012. Impacts of human activities on nutrient transports in the huanghe (Yellow River) estuary. J. Hydrol. 430–431, 103–110.
Liu, J.N., Du, J.Z., Yi, L.X., 2017. Ra tracer-based study of submarine groundwater discharge and associated nutrient fluxes into the Bohai Sea, China: a highly human-affected marginal sea. J. Geophys. Res. Oceans 122 (11), 8646–8660.
Louw, D.C., van der Plas, A.K., Mohrholz, V., Wasmund, N., Junker, T., Eggert, A., 2016. Seasonal and interannual phytoplankton dynamics and forcing mechanisms in the northern Benguela upwelling system. J. Mar. Syst. 157, 124–134.
Lyngsgaard, M.M., Markager, S., Richardson, K., Møller, E.F., Jakobsen, H.H., 2017. How well does chlorophyll explain the seasonal variation in phytoplankton Activity? Estuar. Coasts 40 (5), 1263–1275.
Macias, D., Huertas, I.E., Garcia-Gorriz, E., Stips, A., 2019. Non-redfieldian dynamics driven by phytoplankton phosphate frugality explain nutrient and chlorophyll patterns in model simulations for the Mediterranean Sea. Prog. Oceanogr. 173, 37–50.
Malone, T.C., Conley, D.J., Fisher, T.R., Glibert, P.M., Harding, L.W., Sellner, K.G., 1996. Scales of nutrient-limited phytoplankton productivity in Chesapeake Bay. Estuaries 19 (2), 371–385.
Mills, M.M., Arrigo, K.R., 2010. Magnitude of oceanic nitrogen fixation influenced by the nutrient uptake ratio of phytoplankton. Nat. Geosci. 3 (6), 412–416.
Mu, D., Yuan, D., Feng, H., Xing, F., Teo, F.Y., Li, S., 2017. Nutrient fluxes across sediment-water interface in Bohai Bay Coastal Zone, China. Mar. Pollut. Bull. 114 (2), 705–714.
Ounissi, M., Amira, A.B., Dulac, F., 2018. Riverine and wet atmospheric inputs of materials to a North Africa coastal site (Annaba Bay, Algeria). Prog. Oceanogr. 165, 19–34.
Pan, S.S., Shi, J., Gao, H.W., Guo, X.Y., Yao, X.H., Gong, X., 2017. Contributions of physical and biogeochemical processes to phytoplankton biomass enhancement in the surface and subsurface layers during the passage of Typhoon Damrey. Jo. Geophys. Res. Biogeosci. 122 (1), 212–229.
Pennock, J.R., Boyer, J.N., Herrera-Silveira, J.A., Iverson, R.L., Whitledge, T.E., Mortazavi, B., Comin, F.A., 1999. Nutrient behavior and phytoplankton production in Gulf of Mexico estuaries. Biogeochem. Gulf Mexico Estuar. 109–162.
Purina, I., Labucis, A., Barda, I., Jurgensone, I., Aigars, J., 2018. Primary productivity in the Gulf of Riga (Baltic Sea) in relation to phytoplankton species and nutrient variability. Oceanologia 60 (4), 544–552.
Qi, J.H., Yu, Y., Yao, X.H., Gang, Y., Gao, H.W., 2020. Dry deposition fluxes of inorganic nitrogen and phosphorus in atmospheric aerosols over the marginal seas and Northwest Pacific. Atmos. Res. 245, 105076.
Redfield, A.C., 1934. On the proportions of organic derivations in sea water and their relation to the composition of plankton. In: Daniel, R.J. (Ed.), James Johnstone Memorial Volume. University Press of Liverpool, pp. 177–192.
Rudnick, D.T., Oviatt, C.A., 1986. Seasonal lags between organic carbon deposition and mineralization in marine sediments. J. Mar. Res. 4 (44), 815–837.
Shi, J.H., Gao, H.W., Zhang, J., Tan, S.C., Ren, J.L., Liu, C.G., Liu, Y., Yao, X.H., 2012. Examination of causative link between a spring bloom and dry/wet deposition of Asian dust in the Yellow Sea, China. J. Geophys. Res. Atmos. 117 (D17).
Shi, X.Y., Qi, M.Y., Tang, H.J., Han, X.R., 2015. Spatial and temporal nutrient variations in the Yellow Sea and their effects on Ulva prolifera blooms. Estuar. Coast. Shelf Sci. 163, 36–43.
Shou, W.W., Zong, H.B., Ding, P.X., Hou, L.J., 2018. A modelling approach to assess the effects of atmospheric nitrogen deposition on the marine ecosystem in the Bohai Sea, China. Estuar. Coas. Shelf Sci. 208, 36–48.
Song, N., Wang, N., Lu, Y., Zhang, J., 2016. Temporal and spatial characteristics of harmful algal blooms in the Bohai Sea during 1952–2014. Cont. Shelf Res. 122, 77–84.
Song, G.D., Liu, S.M., Zhang, J., Zhu, Z.Y., Zhang, G.L., Marchant, H.K., Kuypers, M.M.M., Lavik, G., 2020. Response of benthic nitrogen cycling to estuarine hypoxia. Limnol. Oceanogr. 66 (3), 652–666.
Sui, Q., Xia, B., Xie, H.B., Cui, Y., Chen, B.J., Cui, Z.G., Ding, D.S., 2016. Study on temporal and spatial variation of nutrients and evaluation on eutrophication in the seawater of the Bohai Sea in Winter and Spring of 2014. Prog. Fish. Sci. (02), 10–15 (In Chinese with English abstract).
Tan, E., Zou, W.B., Zheng, Z.Z., Yan, X.L., Du, M.G., Hsu, T.C., Tian, L., Middelburg, J.J., Trull, T.W., Kao, S., 2020. Nat. Clim. Change 10 (4), 349–355.
Wakeham, S.G., Lee, C., 1993. Production, transport, and alteration of particulate organic matter in the marine water column. In: Engel, M.H., Macko, S.A. (Eds.), Organic Geochemistry: Principles and Applications. Springer US, Boston, MA, pp. 145–169.
Wang, Q., Guo, X.Y., Takeoka, H., 2008. Seasonal variations of the Yellow River plume in the Bohai Sea: a model study. J. Geophys. Res. Oceans 113 (C8).
Wang, X.L., Cui, Z.G., Guo, Q., Han, X.R., Wang, J.T., 2009. Distribution of nutrients and eutrophication assessment in the Bohai Sea of China. Chin. J. Oceanol. Limnol. 27 (1), 177–183.
Wang, X.C., Ma, H.Q., Li, R.H., Song, Z.S., Wu, J.P., 2012. Seasonal fluxes and source variation of organic carbon transported by two major Chinese Rivers: the Yellow River and Changjiang (Yangtze) river. Glob. Biogeochem. Cycles 26 (2).
Wang, X.J., Jin, C.J., Wang, L.S., Zhang, C.S., 2018. Distribution characteristics and influencing factors of particulate organic carbon in the Yellow Sea and the Bohai Sea in summer of 2016. Haiyang Xuebao 40 (10), 200–208 (In Chinese with English abstract).
Wang, Y.J., Liu, D.Y., Lee, K., Dong, Z.J., Di, B.P., Wang, Y.Q., Zhang, J.J., 2017. Impact of water-sediment regulation scheme on seasonal and spatial variations of biogeochemical factors in the Yellow River estuary. Estuar. Coast. Shelf Sci. 198, 92–105.
Wang, B.D., Xin, M., Wei, Q.S., Xie, L.P., 2018. A historical overview of coastal eutrophication in the China seas. Mar. Pollut. Bull. 136, 394–400.
Wang, J.J., Yu, Z.G., Wei, Q.S., Yao, Q.Z., 2019. Long-term nutrient variations in the Bohai Sea over the past 40 years. J. Geophys. Res. Oceans 124 (1), 703–722.
Wang, Y.B., Sun, Y.Y., Wang, C.X., Chen, W.W., Hu, X.K., 2019. Net-phytoplankton community structure and its environmental correlations in central Bohai Sea and the Bohai Strait. Aquat. Ecosyst. Health Manag. 22 (4), 481–493.
Xin, M., Wang, B.D., Xie, L.P., Sun, X., Wei, Q.S., Liang, S.K., Chen, K., 2019. Long-term changes in nutrient regimes and their ecological effects in the Bohai Sea, China. Mar. Pollut. Bull. 146, 562–573.
Xu, S.S., Song, J.M., Yuan, H.M., Li, X.G., Li, N., Duan, L.Q., Yu, Y., 2011. Petroleum hydrocarbons and their effects on fishery species in the Bohai Sea, North China. J. Environ. Sci. 23 (4), 553–559.
Xu, D.H., Sun, X.M., Chen, B.J., Xia, B., Cui, Z.G., Zhao, J., Jiang, T., Xia, L.C., Qu, K.M., 2016. The ecological characteristics of zooplankton in the central Bohai Sea. Prog. Fish. Sci. 37 (04), 7–18.
Yamaguchi, H., Koga, N., Ichimi, K., Tada, K., 2020. Seasonal variations in phytoplankton productivity in a shallow cove in the eastern Seto Inland Sea, Japan. Fish. Sci. 86 (6), 1067–1078.
Yoshikawa, C., Yamanaka, Y., Nakatsuka, T., 2005. An ecosystem model including nitrogen isotopes: perspectives on a study of the marine nitrogen cycle. J. Oceanogr. 61 (5), 921–942.
Yu, X.J., Guo, X.Y., Gao, H.W., 2020. Detachment of low-salinity water from the yellow river plume in summer. J. Geophys. Res. Oceans 125 (10).
Zhai, W.D., Zhao, H.D., Su, J.L., Liu, P.F., Li, Y.W., Zheng, N., 2019. Emergence of Summertime Hypoxia and Concurrent Carbonate Mineral Suppression in the Central Bohai Sea, China. Journal of Geophysical Research: Biogeosciences 124 (9), 2768–2785.
Zhang, X.L., Wu, Z.M., Li, J., Yu, G.Y., Zhang, Z.N., Gao, S.H., 2006. Modeling study of seasonal variation of the pelagic-benthic ecosystem characteristics of the Bohai Sea. J. Ocean Univ. China 5 (1), 21–28.
Zhang, Y., Yu, Q., Ma, W.C., Chen, L.M., 2010. Atmospheric deposition of inorganic nitrogen to the eastern China seas and its implications to marine biogeochemistry. J. Geophys. Res. 115 (D7).
Zhang, B., Li, Z.Y., Jin, X.S., 2012. Functional groups of fish assemblages and their major species in the Bohai Sea. J. Fish. China 01, 64–72.
Zhang, H.L., Qiu, Z.F., Sun, D.Y., Wang, S.Q., He, Y.J., 2017. Seasonal and interannual variability of satellite-derived chlorophyll-a (2000–2012) in the Bohai Sea, China. Remote Sens. 9 (6), 582.
Zhang, X.L., Zhang, Q.Q., Yang, A.J., Hou, L.J., Zheng, Y.L., Zhai, W.D., Gong, J., 2018. Incorporation of microbial functional traits in biogeochemistry models provides better estimations of benthic denitrification and anammox rates in coastal oceans. J. Geophys. Res. Biogeosci. 123 (10), 3331–3352.
Zhang, C., He, J.Y., Yao, X.H., Mu, Y.C., Guo, X.Y., Ding, X.K., Yu, Y., Shi, J.H., Gao, H.W., 2020. Dynamics of phytoplankton and nutrient uptake following dust additions in the Northwest Pacific. Sci. Total Environ. 739, 139999.
Zheng, L.W., Zhai, W.D., Wang, L.F., Huang, T., 2020. Improving the understanding of central Bohai Sea eutrophication based on wintertime dissolved inorganic nutrient budgets: roles of North Yellow Sea water intrusion and atmospheric nitrogen deposition. Environ. Pollut. 267, 115626.
Zou, L., Zhang, J., Pan, W.X., Zhan, Y.P., 2001. In situ nutrient enrichment experiment in the bohai and Yellow Sea. J. Plankton Res. 23 (10), 1111–1119.
Zhou, L.M., Sun, Y., Zhang, H.H., Yang, G.P., 2018. Distribution and characteristics of inorganic nutrients in the surface microlayer and subsurface water of the bohai and yellow seas. Cont. Shelf Res. 168, 1–10.